Performance Tradeoff in a Unified Passive Radar and Communications System

Batu K. Chalise, *Senior Member, IEEE*, Moeness G. Amin, *Fellow, IEEE*, and Braham Himed, *Fellow, IEEE*

Abstract—Although radar and communication systems so far have been considered separately, recent advances in passive radar systems have motivated us to propose a unified system, capable of fulfilling the requirements of both radar and communications. In this paper, we provide performance tradeoff analysis for a system consisting of a transmitter, a passive radar receiver (RR), and a communication receiver (CR). The total power is allocated for transmitting the radar waveforms and information signals in such a way that the probability of detection (PD) is maximized, while satisfying the information rate requirement of the CR. An exact closed-form expression for the probability of false alarm (PFA) is derived, whereas PD is approximated by assuming that the signal-to-noise ratio corresponding to the reference channel is often much larger than that corresponding to the surveillance channel. The performance tradeoff between the radar and communication subsystems is then characterized by the boundaries of the PFA-rate and PD-rate regions.

Index Terms—Unified system, passive radar, GLRT detector, performance tradeoff, PD-rate and PFA-rate regions.

I. INTRODUCTION

Radar and communication systems utilize similar radio frequency phenomena and are well characterized by similar signal processing and mathematical techniques [1]. However, the objective of a typical communication system is to transfer information from a source to a sink and then recover that information reliably, whereas in radar, the key objective is to detect and track targets. Moreover, the two systems typically use different frequency bands for their operations. Accordingly, these systems have been independently considered and developed as two separate entities. However, the proliferation of wireless devices and the rapid growth in broadband demand render a hybrid approach for the design of the two systems important and necessary. In this regard, some frequency spectrum, e.g., 2-4 GHz range, has been allocated for both radar [3] and communication systems, such as Long Term Evolution (LTE) [2]. However, when operating in the same frequency band, considerable effort is required to minimize the inter-system interference. This interference can be addressed with several means, such as opportunistic spectrum sharing [4], dual-function radar-communications [5], [6], and cooperation between radar and communication systems [7], [8].

As analytical and experimental results behind passive radar systems (PRS) gradually mature, it is increasingly becoming evident that the signals from cell towers and television (TV) stations, also known as illumination sources, can be utilized to efficiently detect and track targets [9], [10]. To this end, several algorithms have been proposed [11]- [13] for detecting, localizing, and tracking targets in PRS. Moreover, detectors based on the generalized likelihood ratio test (GLRT) function have been proposed in [14] for bi-static PRS and in [15]- [16] for multiple-input multiple-output (MIMO) PRS. While these papers [11]- [16] assume multi-frequency networks, the design of the GLRT detectors has been recently proposed in [17] for single-frequency multi-static PRS.

These works demonstrate that the estimation of the non-cooperative transmitters' waveforms remains a major challenge which can significantly affect the performance of the PRS, namely, target detection and tracking. With accurate waveform estimation, the performance of the PRS approaches that of active radars [17]. This motivates the development of PRS as a part of a bandwidth-flexible communication system in which the transmitters no longer remain non-cooperative and assist the radar receiver, through improved resource allocation, in estimating the broadcast signals more efficiently.

In this paper, we provide performance tradeoff analysis for a unified system consisting of a transmitter, a radar receiver (RR), and a communication receiver (CR). Unlike the dual function system [5], where the same signal is used for both functions at the transmitter, the total system power in the underlying system is allocated for transmitting the radar waveforms and information signal with the objective of optimizing the RR's performance (e.g., maximizing the probability of detection (PD) of the target), while satisfying the information rate requirement of the CR. To this end, an exact closed-form expression for the probability of false alarm (PFA) is derived. A closed-form expression for PD is not analytically tractable and as such, its approximate expression is derived assuming the signal-to-noise-ratio (SNR) of the direct path (transmitter to the RR) signal is high. The performance tradeoff between the two systems is conducted by obtaining the boundaries of the PFA-rate and PD-rate regions.

Notations: Upper (lower) bold face letters will be used for matrices (vectors); $(\cdot)^H$, $\mathbf{I}$, $||\cdot||$, and $\Pr\{\}$ denote Hermitian transpose, identity matrix, Euclidean norm for vector/Frobenius norm for matrix, and the probability operator, respectively. $\mathcal{N}_C(\mu, \sigma^2)$, $\mathcal{X}_k^2(\beta)$, and $\Gamma(x)$ denote Gaussian distribution with mean μ and variance σ^2, a Chi-square distribution with k degrees of freedom and non-centrality parameter β, and complete Gamma function, respectively.

B. K. Chalise is with the Department of Electrical Engineering and Computer Science, Cleveland State University, OH 44115, USA (e-mail: b.chalise@csuohio.edu).

M. G. Amin is with the Center of Advanced Communications, Villanova University, PA 19085 (e-mail: moeness.amin@villanova.edu).

B. Himed is with Air Force Research Laboratory, ARFL/RYMD, Dayton, OH 45433, USA, (e-mail: braham.himed@us.af.mil).

II. SYSTEM MODEL AND GLRT DETECTOR

Consider a communication system that supports both communication and radar receivers as shown in Fig. 1. We as-

sume clutter-free noise-only environment considering that the clutter-path signals can be mitigated by applying a variety of techniques (see [15]- [16] and references therein). The trans-
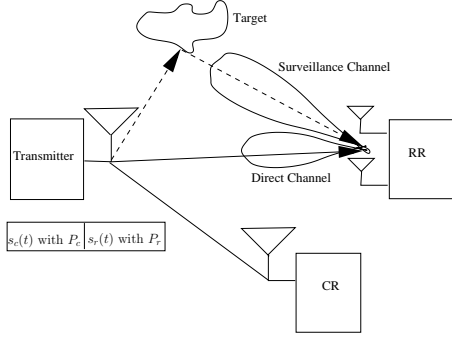

Fig. 1. A unified system with a transmitter, a RR and a CR

mitter uses a portion of the total system power to broadcast a radar waveform $s_r(t)$, whereas the other portion is employed for broadcasting information signal $s_c(t)$. In order to minimize the interference observed by the RR and CR, we consider that the two signal transmissions are scheduled optimally using non-overlapping groups of resource element (time-frequency) units [2]. The tradeoff analysis is conducted by solving an optimization problem, where the objective is to maximize PD of a target at the RR, while ensuring that the information rate for the CR is above a certain threshold value. This problem is expressed as

$$\max_{P_r, P_c} \; P_{\mathrm{D}} \;\; \text{s.t.} \;\; R \geq r_m, P_r + P_c \leq P_T, \quad (1)$$

where P_r and P_c are the power allocated for the information and radar waveforms, respectively, P_T is the total available power, P_{D} denotes probability of detection, R is the information rate for the CR receiver and r_m is the corresponding threshold value. Let γ_C be the instantaneous signal-to-noise ratio (SNR) at the CR. The information rate, in bits per channel use (bpcu), is given by

$$R = \log_2 \left(1 + P_c \gamma_C\right), \quad (2)$$

where we assume that the signal coming through the target path is much weaker than that the direct path from the transmitter. On the other hand, the passive RR utilizes adaptive beamforming to separate the received signal into a reference (transmitter-RR) channel and a surveillance (transmitter-target-RR) channel signals [17]. Assuming that there is a single target, the detection problem turns to a binary hypothesis testing problem. Under the null hypothesis, H_0, and the alternative hypothesis, H_1, the received signals of L time-domain samples are given by [15]- [16]

$$H_0 : \left\{ \begin{array}{c} \mathbf{x}_{\mathrm{d}} = \gamma_{\mathrm{d}} \mathbf{D}_{\mathrm{d}} \mathbf{s}_r + \mathbf{n}_{\mathrm{d}}, \\ \mathbf{x}_{\mathrm{s}} = \mathbf{n}_{\mathrm{s}} \end{array} \right. , \; H_1 : \left\{ \begin{array}{c} \mathbf{x}_{\mathrm{d}} = \gamma_{\mathrm{d}} \mathbf{D}_{\mathrm{d}} \mathbf{s}_r + \mathbf{n}_{\mathrm{d}}, \\ \mathbf{x}_{\mathrm{s}} = \gamma_{\mathrm{t}} \mathbf{D}_{\mathrm{t}} \mathbf{s}_r + \mathbf{n}_{\mathrm{s}} \end{array} \right.$$

where $\mathbf{D}_{\mathrm{d}}$ and $\mathbf{D}_{\mathrm{t}}$ are the $L \times L$ unitary delay-Doppler operator matrices corresponding to the reference and surveillance channels, respectively, and $\mathbf{s}_r$ is the $L \times 1$ vector of sampled radar waveform $s_r(t)$ such that $||\mathbf{s}_r||^2 = P_r$. γ_{d} and γ_{t} are the scalar channel coefficients corresponding to the two channels. The receiver noise at the antennas used for the reference and

surveillance channels are denoted by $\mathbf{n}_{\mathrm{d}}$ and $\mathbf{n}_{\mathrm{s}}$, respectively. In general, γ_{d}, γ_{t}, and $\mathbf{s}_r$ are not known. For a known location of the stationary transmitter, and location and velocity of the target at a hypothesized position (range-Doppler cell), $\mathbf{D}_{\mathrm{d}}$ and $\mathbf{D}_{\mathrm{t}}$ can be computed. Moreover, since $\mathbf{D}_{\mathrm{d}} \mathbf{D}_{\mathrm{d}}^H = \mathbf{D}_{\mathrm{t}} \mathbf{D}_{\mathrm{t}}^H = \mathbf{I}$, the received signals, after unitary transformations with $\mathbf{D}_{\mathrm{d}}$ and $\mathbf{D}_{\mathrm{t}}$ (i.e., $\tilde{\mathbf{x}}_{\mathrm{d}} \triangleq \mathbf{D}_{\mathrm{d}}^H \mathbf{x}_{\mathrm{d}}, \tilde{\mathbf{x}}_{\mathrm{s}} \triangleq \mathbf{D}_{\mathrm{t}}^H \mathbf{x}_{\mathrm{t}}$), simplify to

$$H_0 : \left\{ \begin{array}{c} \tilde{\mathbf{x}}_{\mathrm{d}} = \gamma_{\mathrm{d}} \mathbf{s}_r + \tilde{\mathbf{n}}_{\mathrm{d}}, \\ \tilde{\mathbf{x}}_{\mathrm{s}} = \tilde{\mathbf{n}}_{\mathrm{s}} \end{array} \right. , \; H_1 : \left\{ \begin{array}{c} \tilde{\mathbf{x}}_{\mathrm{d}} = \gamma_{\mathrm{d}} \mathbf{s}_r + \tilde{\mathbf{n}}_{\mathrm{d}}, \\ \tilde{\mathbf{x}}_{\mathrm{s}} = \gamma_{\mathrm{t}} \mathbf{s}_r + \tilde{\mathbf{n}}_{\mathrm{s}} \end{array} \right. , \quad (3)$$

where $\tilde{\mathbf{n}}_{\mathrm{d}} = \mathbf{D}_{\mathrm{d}}^H \mathbf{n}_{\mathrm{d}} \sim \mathcal{N}_C(\mathbf{0}, \sigma^2 \mathbf{I})$ and $\tilde{\mathbf{n}}_{\mathrm{s}} = \mathbf{D}_{\mathrm{t}}^H \mathbf{n}_{\mathrm{s}} \sim \mathcal{N}_C(\mathbf{0}, \sigma^2 \mathbf{I})$. The detection problem is solved by comparing the likelihood ratio test function (LRT), $\Lambda(\tilde{\mathbf{x}}_{\mathrm{d}}, \tilde{\mathbf{x}}_{\mathrm{s}}) = \frac{f((\tilde{\mathbf{x}}_{\mathrm{d}}, \tilde{\mathbf{x}}_{\mathrm{s}})|H_1)}{f((\tilde{\mathbf{x}}_{\mathrm{d}}, \tilde{\mathbf{x}}_{\mathrm{s}})|H_0)}$, with a certain threshold value, γ, which is determined according to a given PFA. $f((\tilde{\mathbf{x}}_{\mathrm{d}}, \tilde{\mathbf{x}}_{\mathrm{s}})|H_1)$ and $f((\tilde{\mathbf{x}}_{\mathrm{d}}, \tilde{\mathbf{x}}_{\mathrm{s}})|H_0)$ denote the joint probability density functions (PDFs) of $\tilde{\mathbf{x}}_{\mathrm{d}}$ and $\tilde{\mathbf{x}}_{\mathrm{s}}$ under the hypotheses H_1 and H_0, respectively. These PDFs are expressed as

$$f((\tilde{\mathbf{x}}_{\mathrm{d}}, \tilde{\mathbf{x}}_{\mathrm{s}})|H_i) = \frac{1}{(\pi \sigma^2)^L} \mathrm{e}^{\frac{-||\tilde{\mathbf{x}}_{\mathrm{d}} - \gamma_{\mathrm{d}} \mathbf{s}_r||^2 - ||\bar{\mathbf{x}}_i||^2}{\sigma^2}}, \quad (4)$$

where $\bar{\mathbf{x}}_i = \tilde{\mathbf{x}}_{\mathrm{s}}$ for $i = 0$ and $\bar{\mathbf{x}}_i = \tilde{\mathbf{x}}_{\mathrm{s}} - \gamma_{\mathrm{t}} \mathbf{s}_r$ for $i = 1$. Since γ_{d}, γ_{t}, and $\mathbf{s}_r$ are unknown, they are substituted with their estimated values in the LRT function. This leads to a new test function known as GLRT. Taking the logarithm of the GLRT function, the maximum likelihood estimates of $\{\gamma_{\mathrm{t}}, \gamma_{\mathrm{d}}, \mathbf{s}_r\}$ can be obtained from

$$\max_{\{\gamma_{\mathrm{t}}, \gamma_{\mathrm{d}}, \mathbf{s}_r\}} \log f((\tilde{\mathbf{x}}_{\mathrm{d}}, \tilde{\mathbf{x}}_{\mathrm{s}})|H_1) - \max_{\{\gamma_{\mathrm{d}}, \mathbf{s}_r\}} \log f((\tilde{\mathbf{x}}_{\mathrm{d}}, \tilde{\mathbf{x}}_{\mathrm{s}})|H_0). \quad (5)$$

Substituting (4) into (5), we can show that

$$\max_{\{\gamma_{\mathrm{d}}, \mathbf{s}_r\}} \log f((\tilde{\mathbf{x}}_{\mathrm{d}}, \tilde{\mathbf{x}}_{\mathrm{s}})|H_0) = \min_{\{\gamma_{\mathrm{d}}, \mathbf{s}_r\}} ||\tilde{\mathbf{x}}_{\mathrm{d}} - \gamma_{\mathrm{d}} \mathbf{s}_r||^2 + ||\tilde{\mathbf{x}}_{\mathrm{s}}||^2,$$

$$\max_{\{\gamma_{\mathrm{d}}, \gamma_{\mathrm{t}}, \mathbf{s}_r\}} \log f((\tilde{\mathbf{x}}_{\mathrm{d}}, \tilde{\mathbf{x}}_{\mathrm{s}})|H_1) = \min_{\{\gamma_{\mathrm{d}}, \gamma_{\mathrm{t}}, \mathbf{s}_r\}} \left\{ ||\tilde{\mathbf{x}}_{\mathrm{d}} - \gamma_{\mathrm{d}} \mathbf{s}_r||^2 + ||\tilde{\mathbf{x}}_{\mathrm{s}} - \gamma_{\mathrm{t}} \mathbf{s}_r||^2 \right\}. \quad (6)$$

Expanding $f_0 \triangleq ||\tilde{\mathbf{x}}_{\mathrm{d}} - \gamma_{\mathrm{d}} \mathbf{s}_r||^2 + ||\tilde{\mathbf{x}}_{\mathrm{s}}||^2$, it can readily be shown that f_0 is minimized by $\gamma_{\mathrm{d}} = \frac{\mathbf{s}_r^H \tilde{\mathbf{x}}_{\mathrm{d}}}{\mathbf{s}_r^H \mathbf{s}_r}$ and $\mathbf{s}_r = \sqrt{P_r} \frac{\tilde{\mathbf{x}}_{\mathrm{d}}}{||\tilde{\mathbf{x}}_{\mathrm{d}}||}$. Substituting these values of γ_{d} and $\mathbf{s}_r$ into f_0, we obtain

$$\max_{\{\gamma_{\mathrm{d}}, \mathbf{s}_r\}} \log f((\tilde{\mathbf{x}}_{\mathrm{d}}, \tilde{\mathbf{x}}_{\mathrm{s}})|H_0) = ||\tilde{\mathbf{x}}_{\mathrm{s}}||^2. \quad (7)$$

On the other hand, for a given $\mathbf{s}_r$, γ_{t} which minimizes $f_1 \triangleq ||\tilde{\mathbf{x}}_{\mathrm{d}} - \gamma_{\mathrm{d}} \mathbf{s}_r||^2 + ||\tilde{\mathbf{x}}_{\mathrm{s}} - \gamma_{\mathrm{t}} \mathbf{s}_r||^2$ is given by $\gamma_{\mathrm{t}} = \frac{\mathbf{s}_r^H \tilde{\mathbf{x}}_{\mathrm{s}}}{\mathbf{s}_r^H \mathbf{s}_r}$, whereas γ_{d} which minimizes f_1 remains the same, i.e., $\gamma_{\mathrm{d}} = \frac{\mathbf{s}_r^H \tilde{\mathbf{x}}_{\mathrm{d}}}{\mathbf{s}_r^H \mathbf{s}_r}$. Accordingly, the remaining minimization of f_1 w.r.t. $\mathbf{s}_r$ is expressed as

$$\min_{\{||\mathbf{s}_r||^2 = P_r\}} \left\{ ||\tilde{\mathbf{x}}_{\mathrm{d}}||^2 + ||\tilde{\mathbf{x}}_{\mathrm{s}}||^2 - \frac{\mathbf{s}_r^H \left(\tilde{\mathbf{x}}_{\mathrm{d}} \tilde{\mathbf{x}}_{\mathrm{d}}^H + \tilde{\mathbf{x}}_{\mathrm{s}} \tilde{\mathbf{x}}_{\mathrm{s}}^H \right) \mathbf{s}_r}{\mathbf{s}_r^H \mathbf{s}_r} \right\}, \quad (8)$$

where the optimum $\mathbf{s}_r$ is obtained by maximizing the term $t \triangleq \frac{\mathbf{s}_r^H \left(\tilde{\mathbf{x}}_{\mathrm{d}} \tilde{\mathbf{x}}_{\mathrm{d}}^H + \tilde{\mathbf{x}}_{\mathrm{s}} \tilde{\mathbf{x}}_{\mathrm{s}}^H \right) \mathbf{s}_r}{\mathbf{s}_r^H \mathbf{s}_r}$, which yields

$$\mathbf{s}_r = \sqrt{P_r} \mathbf{v}_{\max} \left(\tilde{\mathbf{x}}_{\mathrm{d}} \tilde{\mathbf{x}}_{\mathrm{d}}^H + \tilde{\mathbf{x}}_{\mathrm{s}} \tilde{\mathbf{x}}_{\mathrm{s}}^H \right), \quad (9)$$

where $\mathbf{v}_{\max}(\cdot)$ stands for the eigenvector corresponding to the largest eigenvalue of the matrix $\mathbf{A} \triangleq \tilde{\mathbf{x}}_{\mathrm{d}} \tilde{\mathbf{x}}_{\mathrm{d}}^H + \tilde{\mathbf{x}}_{\mathrm{s}} \tilde{\mathbf{x}}_{\mathrm{s}}^H$.

Substituting (9) into (8) and using (7), the GLRT function becomes

$$\log \Lambda(\tilde{\mathbf{x}}_d, \tilde{\mathbf{x}}_s) = \frac{1}{\sigma^2} \left[\lambda_{\max}(\mathbf{A}) - ||\tilde{\mathbf{x}}_d||^2 \right], \qquad (10)$$

where $\lambda_{\max}(\cdot)$ denotes the maximum eigenvalue of $\mathbf{A}$.

III. Radar Performance and Tradeoff Analysis

Since $\mathbf{A}$ is a non-central complex Wishart distributed random matrix, the PDF of $\lambda_{\max}(\mathbf{A})$ is known [15]. On the other hand, $||\tilde{\mathbf{x}}_d||^2$ is a non-central Chi-square distributed random variable. As such, the PDF of the difference $\lambda_{\max}(\mathbf{A}) - ||\tilde{\mathbf{x}}_d||^2$ is not known in closed-form, mainly due to the fact that the two random variables are not statistically independent. Despite this challenge, we first derive in this section an exact closed-form expression of the PFA. The derivation of PD remains analytically intractable, but can be approximated in the case of high direct-path signal-to-noise-ratio (D-SNR).

Since $\mathbf{A}$ is a sum of two rank-one matrices, its eigenvalues can be determined in closed-form. The maximum eigenvalue is expressed as [14]

$$\lambda_{\max}(\mathbf{A}) = \frac{1}{2}\left[||\tilde{\mathbf{x}}_d||^2 + ||\tilde{\mathbf{x}}_s||^2 + \right.$$
$$\left. \sqrt{(||\tilde{\mathbf{x}}_s||^2 - ||\tilde{\mathbf{x}}_d||^2)^2 + 4|\tilde{\mathbf{x}}_d^H \tilde{\mathbf{x}}_s|^2} \right]. \quad (11)$$

Substituting (11) into (10) and after straightforward manipulations, the PFA can be expressed as

$$P_{FA} = \Pr\left\{ \tilde{\mathbf{x}}_s^H \mathbf{B} \tilde{\mathbf{x}}_s \geq \sigma^2 \gamma | H_0 \right\}, \qquad (12)$$

where $\mathbf{B} \triangleq \frac{\tilde{\mathbf{x}}_d \tilde{\mathbf{x}}_d^H + \sigma^2 \gamma \mathbf{I}}{||\tilde{\mathbf{x}}_d||^2 + \sigma^2 \gamma}$. Similarly, PD is expressed as $P_D = \Pr\left\{ \tilde{\mathbf{x}}_s^H \mathbf{B} \tilde{\mathbf{x}}_s \geq \sigma^2 \gamma | H_1 \right\}$. Note that $\tilde{\mathbf{x}}_d$ is the same under both hypotheses, whereas $\tilde{\mathbf{x}}_s = \tilde{\mathbf{n}}_s$ under H_0. The derivation of the PFA is given in (13) (see Appendix), where $\alpha_R = \frac{2|\gamma_d|^2 P_r}{\sigma^2}$ and $_1F_1(a; b; x)$ represents the hypergeometric function [18].

As indicated previously, a closed-form expression for P_D is not tractable. This is due to the fact that, under H_1, $\tilde{\mathbf{x}}_s$ is not zero-mean Gaussian. Consequently, in contrast to the case of H_0, the statistics of the quadratic form $\tilde{\mathbf{x}}_s^H \mathbf{B} \tilde{\mathbf{x}}_s$ depend also on the statistics of the eigenvectors of $\mathbf{B}$ (in addition to that of the eigenvalues of $\mathbf{B}$) . To this end, we approximate PD for high D-SNR, i.e., when $\gamma_R \triangleq \frac{|\gamma_d|^2}{\sigma^2}$ assumes large values. In this case, $\tilde{\mathbf{x}}_d \approx \gamma_d \mathbf{s}_r$, and thus $\mathbf{B}$ can be approximated as

$$\mathbf{B} \approx \frac{\frac{|\gamma_d|^2}{\sigma^2} \mathbf{s}_r \mathbf{s}_r^H + \gamma \mathbf{I}}{\frac{P_r |\gamma_d|^2}{\sigma^2} + \gamma} \approx \frac{\mathbf{s}_r \mathbf{s}_r^H}{P_r}. \qquad (14)$$

In this case, the PD is approximated as

$$P_D \approx \Pr\left\{ \frac{2}{\sigma^2} \tilde{\mathbf{x}}_s^H \frac{\mathbf{s}_r \mathbf{s}_r^H}{P_r} \tilde{\mathbf{x}}_s \geq 2\gamma | H_1 \right\}. \qquad (15)$$

Since $\tilde{\mathbf{x}}_s \sim \mathcal{N}_C(\gamma_t \mathbf{s}_r, \sigma^2 \mathbf{I})$ under H_1 and $\frac{\mathbf{s}_r \mathbf{s}_r^H}{P_r}$ is a rank-one matrix with eigenvalue 1, then $\frac{2}{\sigma^2} \tilde{\mathbf{x}}_s^H \left(\frac{\mathbf{s}_r \mathbf{s}_r^H}{P_r} \right) \tilde{\mathbf{x}}_s \sim \mathcal{X}_2^2 \left(\frac{2|\gamma_t|^2 P_r}{\sigma^2} \right)$. Substituting its PDF into (15), the approximated PD is expressed as

$$P_D \approx Q_1 \left(\sqrt{P_r \gamma_T}, \sqrt{2\gamma} \right), \qquad (16)$$

where $\gamma_T = \frac{|\gamma_t|^2}{\sigma^2}$, $Q_1(a, b)$ denotes the first-order Marcum Q-function with parameters a and b. Under high D-SNR approximation, PFA is approximated as

$$P_{PFA} \approx \Pr\left\{ \frac{2}{\sigma^2} \tilde{\mathbf{x}}_s^H \frac{\mathbf{s}_r \mathbf{s}_r^H}{P_r} \tilde{\mathbf{x}}_s \geq 2\gamma | H_0 \right\}. \qquad (17)$$

Since $\tilde{\mathbf{x}}_s \sim \mathcal{N}_C(\mathbf{0}, \sigma^2 \mathbf{I})$ under H_0, $\frac{2}{\sigma^2} \tilde{\mathbf{x}}_s^H \left(\frac{\mathbf{s}_r \mathbf{s}_r^H}{P_r} \right) \tilde{\mathbf{x}}_s \sim \mathcal{X}_2^2(0)$. As such, (17) is expressed as $P_{PFA} \approx e^{-\gamma}$, which means that $\gamma \approx -\log(P_{PFA})$ for a given PFA.

In the optimization problem (1), the maximum value of P_D is achieved when two inequality constraints are simultaneously active. Thus, substituting (2) in $R = r_m$ and using the relation $P_c = P_T - P_r$, we obtain $P_r = P_T - \frac{1}{\gamma_C}(2^{r_m} - 1)$. The corresponding PD is

$$P_D \approx Q_1 \left(\sqrt{\left(P_T - \frac{1}{\gamma_C}(2^{r_m} - 1) \right) \gamma_T}, \sqrt{2\gamma} \right), \quad (18)$$

which shows the effect of sharing P_T, between the CR and RR, on the detection probability and information rate. In particular, P_D increases monotonically with P_r which increases when r_m decreases.

IV. Numerical Results

In Fig. 2 (left-side), the analytical and simulated values of PFA are plotted for different values of D-SNR, where D-SNR is $\frac{P_r |\gamma_d|^2}{\sigma^2}$. It can be observed from this figure that there exists a perfect matching between the theory and the simulations, which verifies the accuracy of the derived expression for PFA. Moreover, when D-SNR increases, the derived PFA approaches $e^{-\gamma}$. The boundaries of the PFA-rate regions are
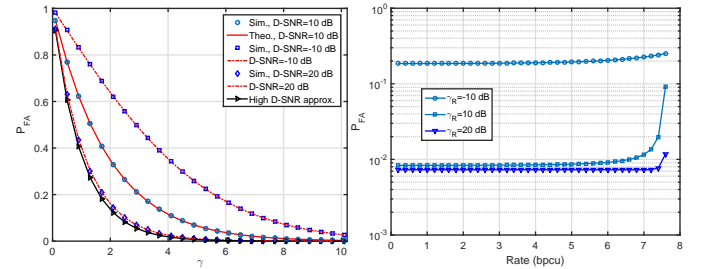

Fig. 2. Left- PFA versus γ (L=10), Right - PFA versus rate ($P_T = 20$ W, $\gamma_C = 10$ dB, $\gamma = 5$, $L = 10$).

shown in Fig. 2 (right-side) for different values of γ_R. When the rate requirement increases, the PFA also increases. The lowest PFA is achieved when the target information rate is minimum. When γ_R increases, PFA approaches the best possible value (in this case it is e^{-5}) and remains almost constant even when the rate requirement increases. For a given P_T, γ_C and γ_T, the boundaries of the PD-rate regions are shown in Fig. 3 (left-side) by changing γ_R. This figure verifies that the accuracy of the approximated PD increases when γ_R increases. In Fig. 3 (right-side), taking the analytical expression of the approximated PD, the PD-rate regions are shown for different values of γ_T. The boundaries of the regions widen when γ_T increases.

$$P_{\text{FA}} = \text{e}^{-\gamma} + \frac{2\gamma \text{e}^{-\left(\gamma + \frac{\alpha_{\text{R}}}{2}\right)}}{2^L \Gamma(L)} \left\{ \sum_{k=0}^{L-2} \sum_{p=0}^{k} \binom{k}{p} 2^{L-1} \gamma^{k-p} \Gamma(L+p-k-1) {}_1F_1 \left(L+p-k-1; L; \frac{\alpha_{\text{R}}}{2} \right) \right.$$

$$\left. - \sum_{k=0}^{L-2} \sum_{l=0}^{k} \sum_{p=0}^{k} \binom{k}{p} \frac{2^{k-p-l} \gamma^{k-p}}{l!} \Gamma(L+l+p-k-1) {}_1F_1 \left(L+l+p-k-1; L; \frac{\alpha_{\text{R}}}{4} \right) \right\}. \tag{13}$$
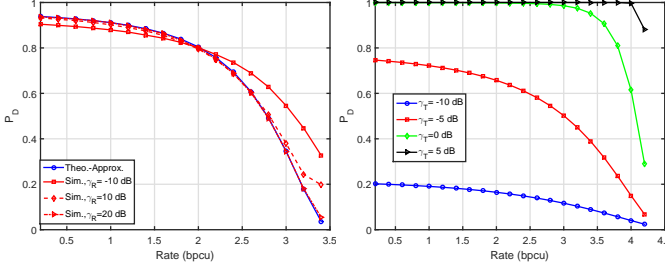

Fig. 3. PD versus rate: Left - $L = 10$, $P_T = 10$ W, $\gamma_T = \gamma_C = 0$ dB, Right - $L = 10$, $P_T = 20$ W, $\gamma_R = 10$ dB, $\gamma_C = 0$ dB.

V. Conclusions

In this paper, we analyzed the performance tradeoff between radar and communication receivers in a unified system consisting of a transmitter, a passive radar receiver, and a communication receiver. The tradeoff was characterized by obtaining the boundaries of the probability of detection (PD) and the probability of false-alarm (PFA) versus the information rate regions. A closed-form expression for PFA was derived, whereas PD is approximated assuming that the SNR corresponding to the reference channel is high. Computer simulations verify the analytical results.

Appendix -Derivation of (13)

The probability of false alarm (PFA) is expressed as $P_{\text{FA}} = \text{Pr}\left\{ \tilde{\mathbf{n}}_{\text{s}}^H \mathbf{U} \mathbf{\Lambda} \mathbf{U}^H \tilde{\mathbf{n}}_{\text{s}} \geq \sigma^2 \gamma \right\}$, where $\mathbf{U}$ is a matrix of eigenvectors and $\mathbf{\Lambda}$ is a diagonal matrix of eigenvalues of $\mathbf{B}$. It is obvious that one eigenvalue of $\mathbf{B}$ is 1, whereas the remaining $L-1$ eigenvalues are equal to $\lambda = \frac{c}{c+||\tilde{\mathbf{x}}_{\text{d}}||^2}$, where $c = \sigma^2 \gamma$. Since $\tilde{\mathbf{n}}_{\text{s}} \sim \mathcal{N}_C(\mathbf{0}, \sigma^2 \mathbf{I})$ and $\mathbf{U}$ is a unitary matrix, $\bar{\mathbf{n}}_{\text{s}} \triangleq \mathbf{U}^H \tilde{\mathbf{n}}_{\text{s}} \sim \mathcal{N}_C(\mathbf{0}, \sigma^2 \mathbf{I})$. Let $\bar{\mathbf{n}}_{\text{s}} = [\bar{n}_{\text{s},1}, \cdots, \bar{n}_{\text{s},L}]^T$, then PFA can be expressed as

$$P_{\text{FA}} = \text{Pr}\left\{ \frac{2|\bar{n}_{\text{s},1}|^2}{\sigma^2} + \lambda \sum_{k=2}^{L} \frac{2|\bar{n}_{\text{s},k}|^2}{\sigma^2} \geq 2\gamma \right\}. \tag{19}$$

Let $X \triangleq \sum_{k=2}^{L} \frac{2|\bar{n}_{\text{s},k}|^2}{\sigma^2}$ and $Y \triangleq \frac{2|\bar{n}_{\text{s},1}|^2}{\sigma^2}$, where $X \sim \mathcal{X}_{2(L-1)}^2(0)$ and $Y \sim \mathcal{X}_2^2(0)$. Then, (19) is expressed as

$$P_{\text{FA}} = 1 - \text{Pr}\left\{ X \leq (2\gamma - Y)Z \right\}, \text{ with } Z \triangleq \frac{c + ||\tilde{\mathbf{x}}_{\text{d}}||^2}{c}.$$

Let $P_{\text{FA}|z}$ be the PFA conditioned on the random variable Z, which is expressed as

$$P_{\text{FA}|z} = 1 - \int_0^{2\gamma} \int_0^{(2\gamma - y)Z} f_X(x) dx \, f_Y(y) dy, \tag{20}$$

where

$$f_X(x) = \frac{x^{L-2} \text{e}^{-\frac{x}{2}}}{2^{(L-1)} \Gamma(L-1)}, \quad f_Y(y) = \frac{1}{2} \text{e}^{-\frac{y}{2}}. \tag{21}$$

Substituting $f_X(x)$ from (21) into (20), and applying [18, eqn. 3.381.1], we get

$$\int_0^{(2\gamma - y)Z} f_X(x) dx = \frac{\gamma_{\text{Lo}} \left(L-1, \frac{(2\gamma-y)Z}{2} \right)}{\Gamma(L-1)}, \tag{22}$$

where $\gamma_{\text{Lo}}(a, x)$ stands for lower-incomplete Gamma function [18]. Substituting $f_Y(y)$ and the series representation for $\gamma_{\text{Lo}} \left(L-1, \frac{(2\gamma-y)Z}{2} \right)$ [18, eqn. 8.352.1], (20) is expressed as

$$P_{\text{FA}|\bar{z}} = \text{e}^{-\gamma} + \frac{\text{e}^{-\left(\gamma + \frac{\bar{Z}}{2}\right)}}{2} \sum_{k=0}^{L-2} \frac{\left(1 + \frac{\bar{Z}}{2\gamma}\right)^k}{2^k k!} \int_0^{2\gamma} (2\gamma - y)^k \text{e}^{\frac{y\bar{Z}}{4\gamma}} dy,$$

where we use $Z = 1 + \frac{\bar{Z}}{2\gamma}$ with $\bar{Z} \triangleq \frac{2||\tilde{\mathbf{x}}_{\text{d}}||^2}{\sigma^2}$. Applying [18, eqn. 3.382.1], $P_{\text{FA}|\bar{z}}$ is written as

$$P_{\text{FA}|\bar{z}} = \text{e}^{-\gamma} + 2\gamma \text{e}^{-\gamma} \sum_{k=0}^{L-2} \frac{(2\gamma + \bar{Z})^k \bar{Z}^{-(k+1)}}{k!} \gamma_{\text{Lo}} \left(k+1, \frac{\bar{Z}}{2} \right). \tag{23}$$

Note that $\bar{Z} \sim \mathcal{X}_{2L}^2(\alpha_{\text{R}})$, where $\alpha_{\text{R}} \triangleq \frac{2|\gamma_{\text{d}}|^2 P_r}{\sigma^2}$. The PDF of $\bar{Z}$ can be expressed in terms of the hypergeometric function ${}_0F_1(; a; x)$ as

$$f_{\bar{Z}}(\bar{z}) = \text{e}^{-\frac{\alpha_{\text{R}}}{2}} {}_0F_1 \left(;, L; \frac{\alpha_{\text{R}} \bar{z}}{4} \right) \frac{\text{e}^{-\frac{\bar{z}}{2}} \bar{z}^{L-1}}{2^L \Gamma(L)}. \tag{24}$$

Utilizing (24), P_{FA} is expressed as

$$P_{\text{FA}} = \int_0^\infty P_{\text{FA}|\bar{Z}} f_{\bar{Z}}(\bar{z}) d\bar{z}. \tag{25}$$

Substituting (23) and (24) into (25), and applying the facts that $\gamma_{\text{Lo}} \left(k+1, \frac{\bar{z}}{2} \right) = k! \left[1 - \text{e}^{-\frac{\bar{z}}{2}} \sum_{l=0}^{k} \frac{\bar{z}^l}{l! 2^l} \right]$ and the binomial expansion, $(2\gamma + \bar{z})^k = \sum_{p=0}^{k} \binom{k}{p} (2\gamma)^{k-p} \bar{z}^p$ [18, eqn. 1.111], (25) can be expressed as

$$P_{\text{FA}} = \text{e}^{-\gamma} + \frac{2\gamma \text{e}^{-\left(\gamma + \frac{\alpha_{\text{R}}}{2}\right)}}{2^L \Gamma(L)} \left\{ \sum_{k=0}^{L-2} \sum_{p=0}^{k} \binom{k}{p} (2\gamma)^{k-p} I_1 - \right.$$

$$\left. \sum_{k=0}^{L-2} \sum_{l=0}^{k} \sum_{p=0}^{k} \frac{1}{l! 2^l} \binom{k}{p} (2\gamma)^{k-p} I_2 \right\}, \tag{26}$$

where, $I_1 = \int_0^\infty \bar{z}^{(L+p-k-1)-1} \text{e}^{-\frac{\bar{z}}{2}} {}_0F_1 \left(;, L; \frac{\alpha_{\text{R}}}{4} \bar{z} \right) d\bar{z}$,

$$I_2 = \int_0^\infty \bar{z}^{(L+l+p-k-1)-1} \text{e}^{-\bar{z}} {}_0F_1 \left(;, L; \frac{\alpha_{\text{R}}}{4} \bar{z} \right) d\bar{z}.$$

Applying [18, eqn. 7.5229] for I_1 and I_2, the expression (13) is obtained.

REFERENCES

[1] M. Davis, "Key Differences between radar and communications systems," *12th Annual International Symposium on Advanced Radio Technologies*, Colorado, July, 2011.

[2] *Evolved Universal Terrestrial Radio Access (E-UTRA); User Equipment (UE) radio transmission and reception*, 3GPP TS 36.101 version 10.3.0 Release 10.

[3] A. Elston, "Coexistence of S band radar systems with future mobile services operating in the adjacent 2600MHz band A Brief," *Tech. Rep.*, Clear Mobitel, 2011.

[4] R. Saruthirathanaworakun, J. Peha, and L. Correia, "Performance of data services in cellular networks sharing spectrum with a single rotating radar," in *IEEE International Symposium on a World of Wireless, Mobile and Multimedia Networks (WoWMoM)*, pp. 16, 2012.

[5] S. D. Blunt, P. Yatham, and J. Stiles, "Intra-pulse radar embedded communications," *IEEE Trans. Aerospace and Electronic Systems*, vol. 46, no. 3, pp. 1185-1200, July 2010.

[6] A. Hassanien, M. G. Amin, Y. D. Zhang, and F. Ahmad, "A dual function radar-communications system using sidelobe control and waveform diversity," in *Proc. 2015 IEEE Int. Radar Conf. (RadarCon 2015)*, Arlington, VA, May 2015.

[7] S .C. Surender, R. M. Narayanan, and C. R. Das, "Performance analysis of communications & radar coexistence in a covert UWB OSA system," in *Proc. IEEE Global Commun. Conf., (GLOBECOM 2010)*, Miami, FL, Dec. 2010, pp. 15.

[8] B. Li, A. P. Petropulu, and W. Trappe, "Optimum design for coexistence between matrix completion based MIMO radars and a MIMO communication system," *IEEE Trans. Signal Process.*, vol. 64, no. 17, pp. 4562-4575, Sept. 2016.

[9] D. Poullin, "Passive detection using digital broadcasters (DAB, DVB) with COFDM modulation," *IEE Proceedings Radar, Sonar and Navigation*, vol. 152, no. 3, pp. 143-152, 2005.

[10] A. A. Salah, R. S. A. Raja Abdullah, A. Ismail, F. Hashim, C. Y. Leow, M. B. Roslee, and N. E. A. Rashid, "Feasibility study of LTE signal as a new illuminators of opportunity for passive radar applications," *IEEE International RF and Microwave Conference (RFM)*, 2013.

[11] B. K. Chalise, Y. D. Zhang, M. G. Amin, and B. Himed, "Target position localization in a passive radar system through convex optimization," in *Proc. SPIE Defense, Security, and Sensing*, vol. 8753, May 2013.

[12] B. K. Chalise, Y. D. Zhang, M.G. Amin, and B. Himed, "Target localization in a multi-static passive radar system through convex optimization," *Signal Processing*, vol. 102, pp. 207-215, Sep. 2014.

[13] S. Subedi, Y. D. Zhang, M. G. Amin, and B. Himed, "Motion parameter estimation of multiple ground moving targets in multi-static passive radar systems," *Eurasip Jrn. Adv. Sig. Process.*, 2014:157.

[14] G. Cui, J. Liu, H. Li, and B. Himed, "Signal detection with noisy reference for passive sensing," *Signal Process.*, no. 108, pp. 389-399, 2015.

[15] D. E. Hack, L. K. Patton, B. Himed, and M. A. Saville, "Centralized passive MIMO radar detection without direct-path references," *IEEE Trans. Signal Process.*, vol. 62, no. 11, June 2014.

[16] D. E. Hack, "Passive MIMO radar detection," *PhD Thesis*, Air Force Institute of Technology, OH, 2013.

[17] B. K. Chalise and H. Himed, "Target detection in single frequency multi-static passive radar systems," in Proc. *IEEE Radar Conference*, Seattle, May 2017, Available at: https://sites.google.com/site/batuchaliseshomepage/publications.

[18] I. S. Gradshteyn and I. M. Ryzhik, *Table of Integrals, Series, and Products*, Academic Press, 2000.